Available online at www.sciencedirect.com
ScienceDirect
Trans. Nonferrous Met. Soc. China 28(2018) 1176−1185
Transactions of Nonferrous Metals Society of China
www.tnmsc.cn

Effect of WS_2 particle size on mechanical properties and tribological behaviors of Cu−WS_2 composites sintered by SPS

Jin ZHOU[1], Chao MA[2], Xiao KANG[1], Lei ZHANG[1], Xin-li LIU[1]

1. State Key Laboratory of Powder Metallurgy, Central South University, Changsha 410083, China;
2. Shanghai Aerospace Systems Engineering Institute, Shanghai 201109, China

Received 18 January 2017; accepted 4 March 2018

Abstract: The mechanical properties and tribological behaviors of Cu−WS_2 composites fabricated by spark plasma sintering (SPS) using two different WS_2 particle sizes of 0.6 and 5.0 μm and Cu powders as raw materials were investigated. The results indicate that the bending strength and tribological behavior of Cu−WS_2 composites are greatly affected by the size of WS_2 particles. The bending strength of Cu−WS_2 composites with the WS_2 particle size of 5.0 μm is 292.2 MPa. As the size of WS_2 particle decreases to 0.6 μm, the bending strength also decreases to 181.5 MPa. Moreover, as the WS_2 particle size decreases from 5.0 to 0.6 μm, the wear rate of Cu−WS_2 composite sharply increases from 2.99×10^{-14} to 6.13×10^{-14} $m^3/(N\cdot m)$ and its friction coefficient increases from 0.158 to 0.172. The size of WS_2 particle (5.0 μm) plays an important role in forming transfer film formed on the counter-face. The sample with 5.0 μm WS_2 particle forms smoother and more continuous transfer film, which results in a low wear rate and friction coefficient of the Cu−WS_2 composites.

Key words: Cu−WS_2 composites; mechanical properties; wear rate; friction coefficient; continuous transfer film; spark plasma sintering

1 Introduction

Copper-based composites containing the solid lubricants have been widely used in many applications, such as brushes, contact strips, bearings as well as motion mechanisms in space [1−3] because of their excellent thermal, electrical conductivities and lubricating properties. Particularly, the effects of different solid lubricants (graphite, MoS_2, WS_2, etc) on the tribological behavior of copper-based composites have been studied extensively [4−6]. However, researches on copper-based composites with WS_2, as a single-phase lubricant, are rarely reported. WS_2 possesses excellent thermal, oxidative stabilities and lubricity [7,8]. Therefore, the tribological behavior of copper-based composites using WS_2 as a single-phase lubricant has high research value. However, WS_2 is prone to react with copper at temperatures higher than 769 °C and it is also broken down easily at a relatively low temperature [9], which are disadvantageous to the lubricity and wear resistance of the composites. Although some researchers have reported that the reaction between copper and a small amount of WS_2 can enhance the bonding of matrix and lubricating phase [10]. However, it is difficult to control the processing of reaction favoring the tribological property of composites. It is well known that the spark plasma sintering (SPS) as a novel sintering technique has been widely used in the field of metal-matrix composites [11]. The SPS technology, compared with the traditional sintering technology, can reduce the sintering temperature in a certain range and notably decrease the sintering time, which may restrain the reaction. Thus, SPS technology is used to prepare the Cu−WS_2 composites in this paper.

The tribological behavior of composites is closely related to the type, spatial distribution and particles size of the lubricating phase. Many researchers [6,12] attempted to study the influence of these factors on the tribological behavior of copper-based composites. For example, CAO et al [10] reported that the Cu−WS_2 composites had a better tribological behavior than the

Foundation item: Projects (51674304, 51604305) supported by the National Natural Science Foundation of China; Project (2016M592445) supported by the China Postdoctoral Science Foundation
Corresponding author: Lei ZHANG; E-mail: zhanglei@csu.edu.cn
DOI: 10.1016/S1003-6326(18)64755-7

Cu−graphite composites. RAJKUMAR et al [13] found that the severe agglomeration of lubricant particles resulted in deterioration of tribological behavior. A few researchers also reported that the tribological properties of composites were remarkably affected by the particle size of lubricant particles [14,15]. Generally, the lubricant with the micron size of 5−400 μm was extensively used to prepare the copper-based composites for exploring its self-lubrication property [16−18]. RAPOPORT et al [19] showed the better tribological properties of Cu−WS_2 composites containing 120 nm fullerene-like WS_2 particles when compared to Cu−WS_2 composites containing micron WS_2 particles. KOÁČIK et al [12] reported the excellent tribological properties of copper−graphite composites with 16 μm graphite. However, JHA et al [20] found that the tribological behaviors of self-lubricating composites were deteriorated by adding 50 μm graphite. Therefore, the optimal size of lubricant in the composites has not been well studied and needs to be deeply clarified. The researches about the effect of WS_2 size on the mechanical properties and tribological behavior of Cu−WS_2 composites are rather limited. Therefore, it is of great significance to further investigate the WS_2 particle size on tribological behavior of Cu−WS_2 composites.

In this work, the Cu−WS_2 composites with WS_2 particle sizes of 5.0 and 0.6 μm were fabricated by SPS, and mechanical properties and tribological behaviors were investigated. The role of WS_2 particle size in the tribological behavior was researched. The morphologies of worn surface, wear debris and sub-surface were observed. Besides, the effect of WS_2 particle size on the tribological behavior of Cu−WS_2 composites was revealed by analyzing the transfer film on counter-face.

2 Experimental

2.1 Preparation of Cu−WS_2 composites

Commercially available electrolytic copper powders with an average particle size of 25 μm were used as matrix material. WS_2 powders with grain sizes of 0.6 and 5.0 μm were selected as a solid lubricant in this work. Two distribution curves of WS_2 particles with different sizes were obtained by the laser particle analyzer, as shown in Fig. 1. Cu powders and WS_2 powders (20%, mass fraction) were mixed in a milling tank for 24 h at a speed of 50 r/min. The mixed powders were then poured into a 40 mm diameter graphite die and sintered using an SPS system (FCT Systeme GmbH Gewerbepark 1696528 Rauenstein, Germany) under Ar atmosphere. The sintering parameters are as follows: 1) raising from room temperature to 650 °C with 100 °C/min under 15 MPa; 2) holding at 650 °C with the pressure of 45 MPa; 3) cooling down to room temperature in 10 min with an on/off pulse sequence of 12:2. The Cu−WS_2 composites with the WS_2 particle sizes of 0.6 and 5.0 μm are referred to as sample S0.6 and sample S5, respectively.

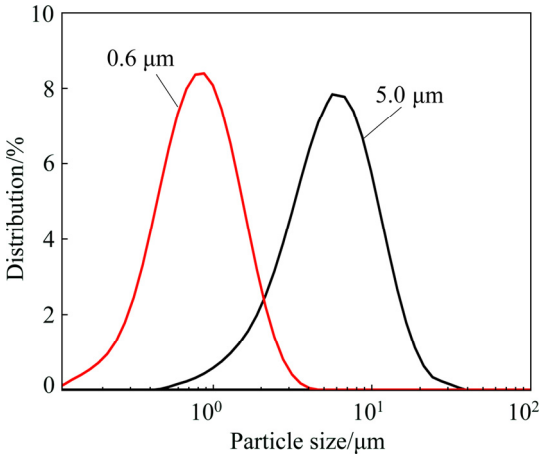

Fig. 1 Two distribution curves of WS_2 particles with different sizes

2.2 Friction and wear tests

The friction and wear tests in this work were implemented on a pin−disc apparatus (CSM Instruments, Peseux, Switzerland). The counter-face disc is Cu5Pb5Zn5Sn alloy with the hardness of HB 145. The size of sample was 3 mm × 6 mm × 6 mm. Then, the surfaces of sample and disc were polished using 1000 and 2000 grit SiC papers. The sliding tests were conducted in air ambient ((25±2) °C and 50%−60% relative humidity). The sliding speed and applied load were 0.92 m/s (500 r/min) and 5 N, respectively, and the sliding distance was 10 km. The mass loss of sample before and after wear test was weighed by the digital microbalance (0.1 mg precision, model TE214S, Sardo-rius, Germany). The wear rate was calculated by the following function:

$$W=\Delta m/(P\rho s) \quad (1)$$

where W is the wear rate; Δm is the wear mass loss; P is the normal load; ρ and s are the density of specimens and sliding distance, respectively.

The relative density of samples was measured according to Archimedes methods, and the bending strength was obtained using standard testing equipment (Instron 3369 testing system, USA). X-ray diffractometry (XRD) was used to reveal the phases of samples. The microstructure, wear morphology and subsurface region were characterized by a field emission scanning electron microscope (FEI, Nova Nano SEM 230). The worn surfaces were analyzed by X-ray photoelectron spectroscopy (XPS-Escalab210). At least, three parallel samples were tested, and the average values were reported.

3 Results and discussion

3.1 Characterization of Cu−WS_2 composite

The XRD patterns of Cu−WS_2 composites after SPS are presented in Fig. 2. It is observed that the peaks can only be indexed to Cu (JCPDS No. 04−0836) and WS_2 (JCPDS No. 08−0237) phases, which confirms that no chemical reaction was generated between Cu and WS_2 during the process of SPS. As a result, the Cu−WS_2 composites with high purity are fabricated due to the special sintering mechanism of SPS. Generally, the copper and WS_2 particles are easily influenced by oxygen, and oxidation occurs at a relatively low temperature [8,21]. In addition, without exposure to the oxygen, the copper and WS_2 could be involved in a chemical reaction when the temperature is higher than 769 °C [9], which is the main reason for few reports about Cu−WS_2 composites. It is difficult to fabricate the high purity Cu−WS_2 composites by traditional sintering process. Fortunately, the chemical reaction between metal and lubricant does not take place during SPS sintering process, which could be attributed to the lower sintering temperature (650 °C), faster heating rate, and shorter holding time of SPS than traditional sintering process.

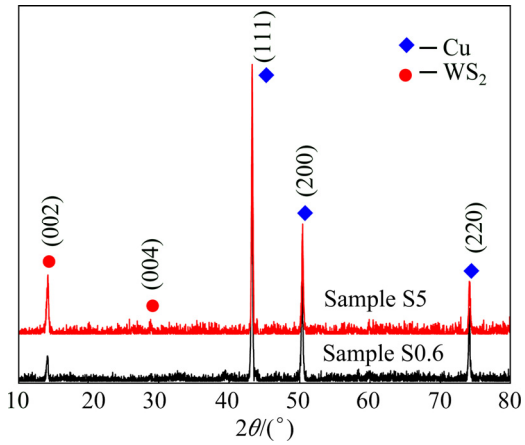

Fig. 2 XRD patterns of samples S0.6 and S5 sintered by SPS

Figure 3 shows the microstructures of samples sintered by SPS. As seen in Fig. 3(a), the arrangement of WS_2 particles in sample S5 presents a long strip distribution. It may be due to the fact that larger particles have better liquidity and are easy to move in the process of SPS. The long strip distribution of WS_2 disappears and large granulated WS_2 particles are found in sample S0.6, as shown in Fig. 3(b). It is found that the distribution of 0.6 μm WS_2 in copper substrate is better than that of 5.0 μm WS_2 from Figs. 3(c) and (d). Compared with

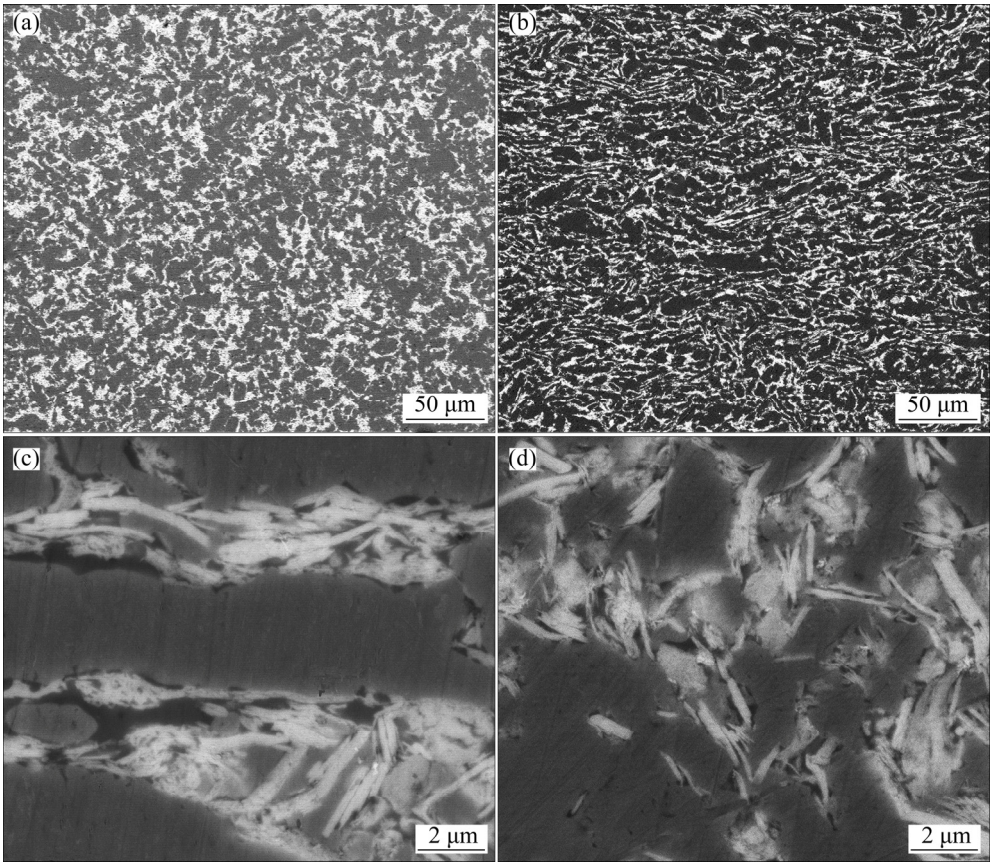

Fig. 3 BSED images of sample sintered by SPS: (a) Sample S5; (b) Sample S0.6; (c) High magnification of (a); (d) High magnification of (b)

5.0 μm WS_2, 0.6 μm WS_2 with same mass fraction has larger number of particles and higher surface energy. Hence, 0.6 μm WS_2 has larger interfacial area with copper substrate, resulting in the lower interfacial combination of sample S0.6.

3.2 Mechanical properties of Cu−WS_2 composites

The mechanical properties of samples with different WS_2 particle sizes are presented in Table 1. Although the relative density of sample S5 and sample S0.6 apparently has less obvious fluctuation, the relative density of Sample S5 is slightly higher than that of sample S0.6. It could be attributed to inferior sintering performance of sample S0.6, resulting in more holes between Cu and WS_2 particles. Sample S5 exhibits higher mechanical properties compared to sample S0.6. The bending strength of sample S5 is 292.2 MPa. As the size of WS_2 particle decreases to 0.6 μm, the bending strength decreases to 181.5 MPa. As known, the number of WS_2 particles with 0.6 μm is larger than that with 5.0 μm WS_2 for the same mass fraction. In addition, the WS_2 particles could be considered as defects in copper-based composites. The defects increase with the increasing amount of WS_2 particles, which deteriorate the sintering between Cu and WS_2 particles, resulting in inferior mechanical properties. As a result, sample S5 has better mechanical properties than sample S0.6. To further understand the difference of mechanical properties between sample S5 and sample S0.6, their SEM fracture morphologies after bending strength tests are shown in Fig. 4. The analogous layered structures considered as flake-like WS_2 particles are presented in Fig. 4(a), which corresponds to Fig. 3(a). The large WS_2 particles with better liquidity are easier to generate rearrangement under the effect of uniaxial pressure and electrical field during the process of SPS, which contributes to the formation of analogous layered structure. Moreover, a large number of dimples are observed. However, the layered fracture morphology disappears, and the distribution of WS_2 particles is disorderly, as shown in Fig. 4(b). The dimples reveal that the bonding strength between the copper particles of sample S5 is strong, which is responsible for the increase in bending strength. Moreover, it is believed that the analogous layered structure could notably improve mechanical properties [22]. The WS_2 particles could be considered as defects in composites. Microcracks are easy to form and propagate at the interface of composites. However, the analogous layered structure impedes the propagation of cracks [22]. In other words, the distance of travel of the two crack tips is approximately equal in the interval of two WS_2 layers, resulting in difficult propagation of crack. Therefore, the propagation of cracks is restrained by the dimples and the analogous layered structure, which plays a significant role in increasing bending strength of sample S5.

Table 1 Mechanical properties of Cu−WS_2 composites with different sizes of WS_2 particles

Sample	Relative density/%	Bending strength/MPa	Brinell hardness (HB)
S5	93.9	292.2	96.3
S0.6	92.8	181.5	91.1

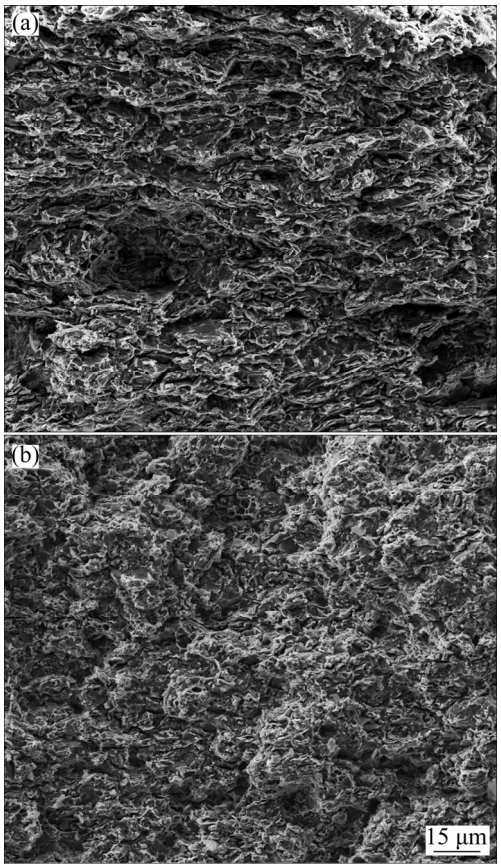

Fig. 4 SEM images of fracture surfaces of sample S5 (a) and sample S0.6 (b) after bending strength tests

3.3 Friction and wear behavior

The friction coefficient curves of sample S5 and sample S0.6 as a function of sliding distance are shown in Fig. 5. As seen from Fig. 5, the friction coefficient curves are also subjected to two stages, a running-in stage and a steady stage. In the running-in stage, the friction coefficient is high because the way of sliding contact between the composites and disc is metal to metal [7]. Subsequently, the friction coefficient decreases with the increase of sliding distance, and then reaches a steady stage. This could be attributed to the release of WS_2 from the composites and the formation of a lubricating film on the counter-face [23]. In addition, it can be seen that sample S5 provides a better lubrication performance than sample S0.6 from the friction coefficient curves. The average friction coefficient in the

steady stage and the wear rate of two composites are displayed in Fig. 6. The average friction coefficients of sample S5 and sample S0.6 are only 0.158 and 0.172, respectively. Importantly, the wear rate of sample S5 is 2.99×10^{-14} $m^3/(N\cdot m)$, which decreases by 51.2% compared with that of sample S0.6 with the wear rate of 6.13×10^{-14} $m^3/(N\cdot m)$. As known, the lubricating behavior of WS_2 derives from its intermechanical weakness which is intrinsic to its crystal structure. When sliding in humid air, the dangling and unsaturated bonds on the edge of basal planes of WS_2 are prone to react with moisture and oxygen in the environment to form tribooxidation products, such as WO_3 [24,25]. SLINEY [26] also reported that the WS_2 in air was oxidized to WO_3 at relatively high temperature. Analyses of the transfer films and wear scars using X-ray photo-electron and laser Raman spectroscopy [27] revealed that the possibility of oxidation of WS_2 to WO_3 during sliding in air is high. Compared with sample S5, sample S0.6 with the same mass fraction has larger number of particles and higher surface energy. Thus, sample S0.6 is more likely to react with moisture and oxygen and form more tribooxidation products on the counter-face during the sliding process. This will result in higher coefficient friction and wear rate. As a result, WS_2 with particle size of 5.0 μm could fully fulfill its intrinsic lubrication, whereby, sample S5 attains better tribological properties and extends its working life.

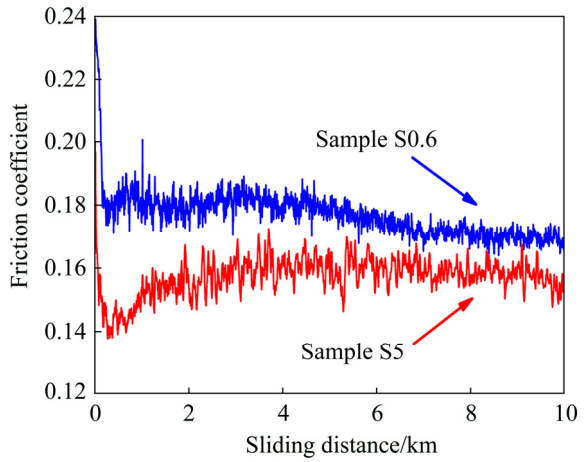

Fig. 5 Friction coefficients of Cu−WS_2 composites with different sizes of WS_2 particles as function of sliding distance

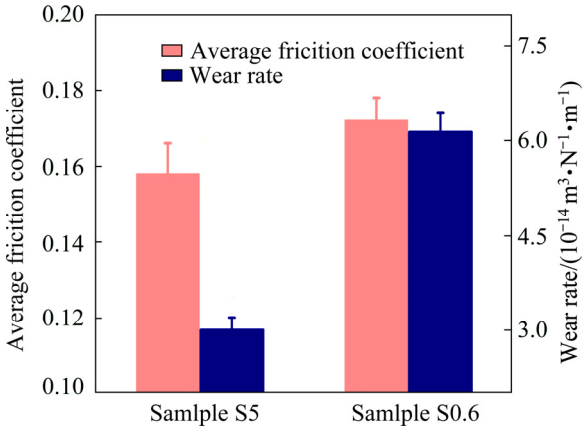

Fig. 6 Average friction coefficients and wear rates of Cu−WS_2 composites with different sizes of WS_2 particle

SEM morphologies of the worn surface of Cu−WS_2 composites are shown in Fig. 7. According to this figure, the worn surfaces of composites are subjected to severe plastic deformation. The wide and shallow grooves on the worn surface of sample S5 can be seen in Fig. 7(a), which accounts for the hardening of wide and continuous transfer film formed on the counter-face during the process of sliding. However, it can be seen that a mass of sheets are peeled off from the worn surface and cracks at the edge of the shallow grooves are formed in Fig. 7(b), which impede the formation of a tribofilm on the worn surface to some extent. This is the reason for the fact that sample S0.6 has a higher friction coefficient than sample S5. It is confirmed that the appearance of wear debris and the wear loss of the composite have a close relation with the morphologies of the worn surfaces [28]. In addition, the sheets shown in Fig. 7 illustrate that the wear mechanism of sample S5 and sample S0.6 is delamination wear in spite of the appearance of grooves. The low friction coefficient of the composite indicates the formation of WS_2 film. According to the report of ZHANG et al [23], XPS analysis can determine the thickness of the worn surface WS_2 film. XPS analysis of the worn surface of sample S5 is presented in Fig. 8. The mole fraction of W on the outmost surface is 17.6%, which is 2.5 times higher than that in the matrix of the composite as shown in Fig. 8(a). Similarly, the mole fraction of S on the outmost surface is 31.7%, about 4.7 times higher than that in the matrix of the composite as displayed in Fig. 8(b). From the mole fractions of W, S and other elements detected by XPS, the mass fractions of W, S and other elements can be calculated. Therefore, it is calculated that about 57% of the worn surface area is covered by WS_2 film. The WS_2 is transferred in the form of film along the sliding direction and completely smears in the contact zone with normal load and eventually forms the WS_2 films. The enrichment of WS_2 on worn surface area remarkably reduces the level of frictional force and number of metal-to-metal contact zone, resulting in the decrease of the friction coefficient and wear rate. In addition, the thickness of the lubricating film is also measured by ion etching technique affiliated with XPS. The accumulated ion etching time is in the scope of 0−120 s, and the etch rate is about 0.66 nm/s. It is found that the intensities of W 4f and S 2p peaks decrease with the increase of etching time. More importantly, the XPS profiles do not change apparently when the accumulated ion etching time exceeds 60 s.

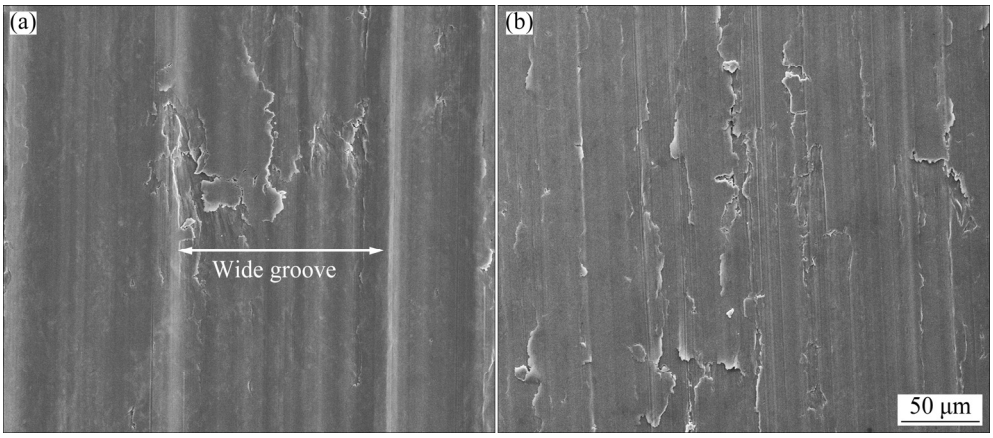

Fig. 7 SEM images of worn surfaces: (a) Sample S5; (b) Sample S0.6

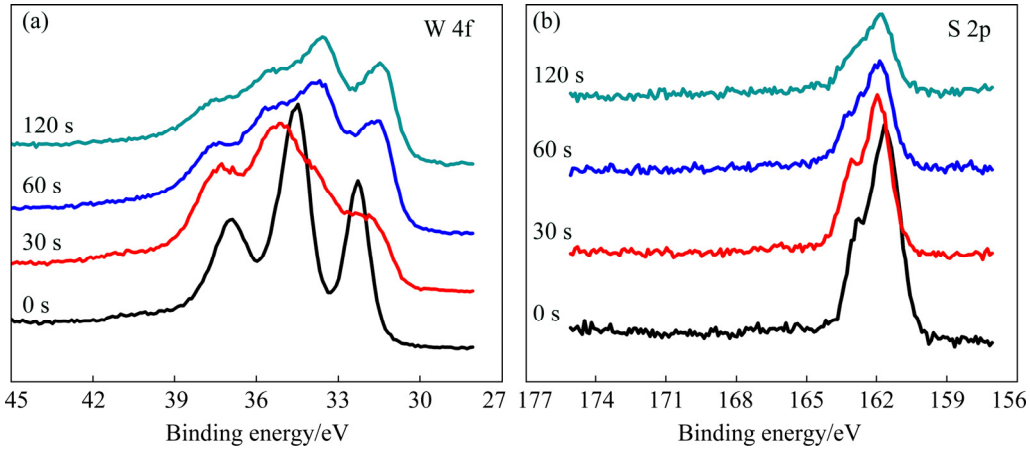

Fig. 8 XPS profiles of W 4f (a) and S 2p (b) on worn surface of sample S5

Hence, it is deduced that the thickness of the WS_2 film in sample S5 is nearly 40 nm.

The wear mechanism is speculated by studying the types of wear debris. Figure 9 displays the SEM micrographs of the collected wear debris of sample S5 and sample S0.6. The primary morphologies of the wear debris are sheet-like, indicating that delamination wear is the dominating wear mechanism in both two composites. The main morphology of wear debris for sample S5 is flake and the particle size is very small. However, the size of most the wear debris for sample S0.6 is more than 100 μm. It is believed that the size of wear debris has a direct relation with wear performance of composites [29]. EDS analysis shows that the total contents of W and S in sample S5 and sample S0.6 are 20.96% and 19.47% (Figs. 9(b) and (d)) respectively, which are close to those of the Cu−WS_2 composites (20% WS_2). Moreover, the sheets and the cracks observed on the worn surfaces provide a worthy evidence for the formation of sheet-like debris. The morphologies of wear debris (Figs. 9(a) and (c)) are in good conformity with those of the worn surfaces (Figs. 7(a) and (b)). By virtue of lower bending strength of sample S0.6, the cracks are easier to form and propagate during the plastic deformation, resulting in large sheet-like debris delaminated from the sliding surfaces. As a result, the wear rate of the composite increases. The number of WS_2 particle with small size is more than that of WS_2 with large size for the same mass fraction. Hence, sample S0.6 obtains more interfacial area between Cu and WS_2 particles. Additionally, the bonding between Cu and WS_2 particles is mechanical bonding, which accelerates the velocity of crack initiation and propagation, making the exfoliation of surface material more easily. It can be known that the size of wear debris of sample S0.6 is much larger than the size of WS_2 and copper particles in copper matrix. Thus, it is believed that the surface material has undergone severe plastic deformation before peeling off as wear debris. In a word, a large number of copper phase and WS_2 particles on the surface and sub-surface undergo severe plastic deformation, resulting in larger wear debris of sample S0.6. In addition, the details of wear debris for sample S5 composite are analyzed as presented in Fig. 9(e). It can be seen that the appearance of smeared WS_2 particles is also observed on the surfaces of wear debris, which provides supporting evidence for

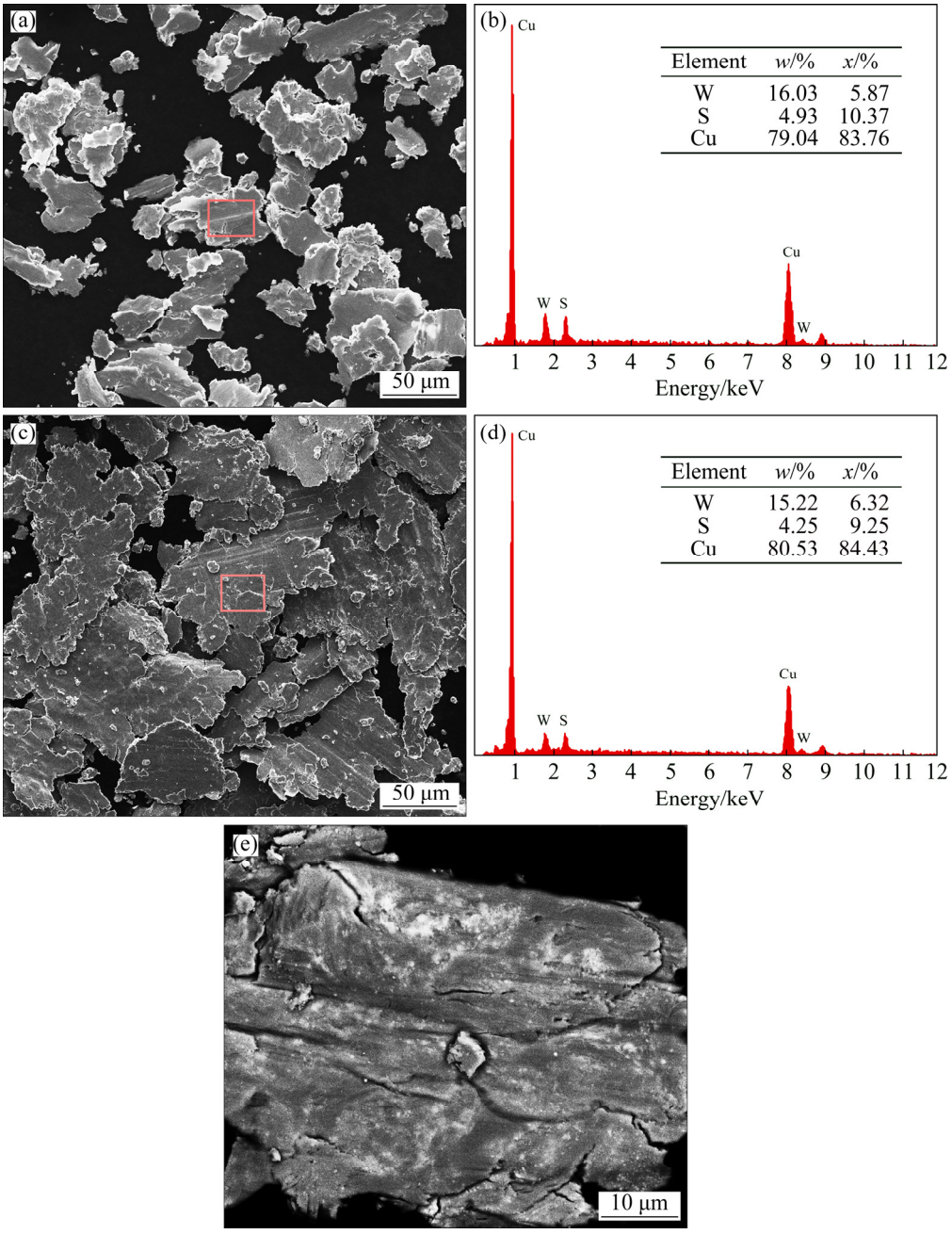

Fig. 9 SEM images of wear debris (a, c, e) and corresponding EDS results (b, d): (a) Sample S5 at 5.0 N; (b) EDS result of region in (a); (c) Sample S0.6 at 5.0 N; (d) EDS result of region in (c); (e) High magnification BSED image of sample S5 at 5.0 N

the formation of a lubricating film on the worn surface and the enrichment of WS_2 on the transfer film on the counter-faces, resulting in the decrement of the friction coefficient and wear rate.

The formation of transfer film on the counter-face remarkably affects the friction and wear behavior of the pin [30,31]. Therefore, the micrographs of transfer film are also detected as shown in Fig. 10. It can be seen that the counter-face is covered by a layered microstructure. Moreover, EDS analysis (Figs. 10(c) and (d)) shows that the composition of the layered microstructure is close to that of the Cu−WS_2 composite, indicating that the transfer film is formed on the counter-face by the removal of materials. It should be noted that the flake-like debris evolves into the continuous transferred layers by repeated compaction and severe plastic deformation under the normal load as illustrated in Fig. 10(a); however, the discontinuous transfer film is observed as shown in Fig. 10(b). The formation of wide and continuous transfer film is likely attributed to the fact that fine and thin wear debris adheres to the counter-face [32]. The wide and continuous transfer film avoids the direct contact between composites and counter-face, which reduces the friction and wear during sliding wear.

In addition, the surface of the wear debris is accumulated with WS_2 lubricating film as illustrated in Fig. 9(e). So, a mass of lubricants are enriched in transfer film. Due to more smooth and continuous transfer films in sample S5, sample S5 obtains better lubricating condition than sample S0.6 in their steady stage. CHEN et al [33] also reported that a good lubrication is obtained due to smoother and more continuous transfer films. It is believed that the smooth and continuous transfer layers contribute to the decrease of friction and wear.

The morphologies of cross section of worn surfaces of the Cu−WS_2 composites are revealed for understanding the formation process of the tribo-layers, as shown in Fig. 11. As can be seen, the WS_2 particles tend to distribute along the sliding direction, which could be attributed to the influence of directional compressive stress and shear stress, resulting in the directional plastic deformation during the process of sliding. The WS_2 particles are extruded gradually from the subsurface of copper matrix to contact surface by this synchronized

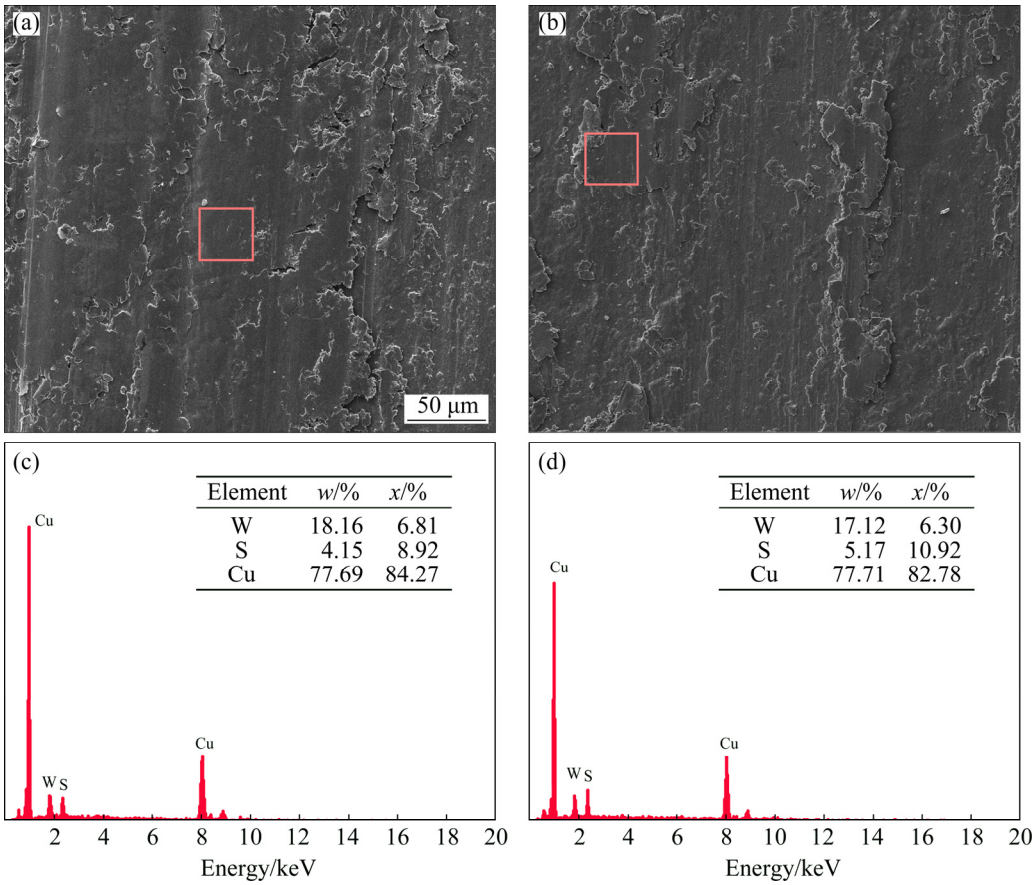

Fig. 10 SEM images of transfer layer on counter-faces (a, b) and corresponding EDS results (c, d): (a) Sample S5; (b) Sample S0.6; (c) EDS result of region in (a); (d) EDS result of region in (b)

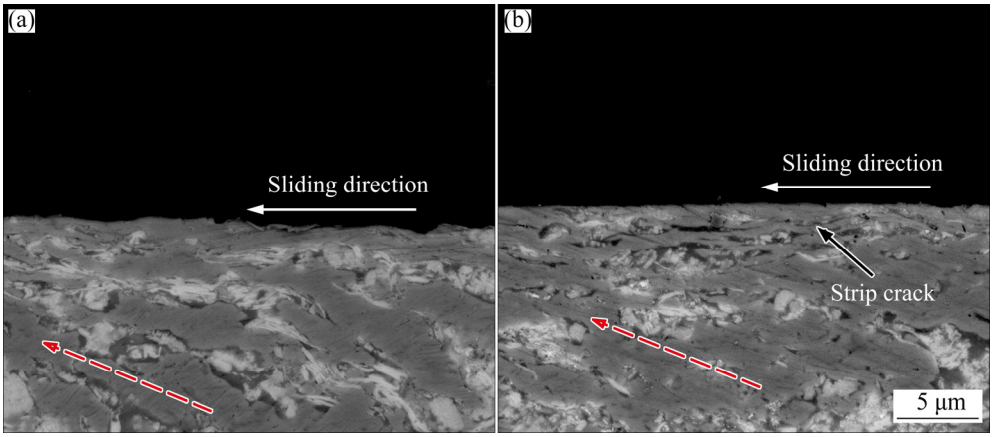

Fig. 11 SEM images of cross section of worn subsurfaces: (a) Sample S5; (b) Sample S0.6

deformation. These extruded WS_2 particles smear on the sliding surface along the sliding direction and then form the WS_2 tribo-layers. It is observed that few cracks are formed on the subsurface of sample S5, as shown in Fig. 11(a). By contrast, longer cracks, parallel to the sliding direction, are observed at the interface of matrix and lubricant, as shown in Fig. 11(b). Therefore, during the process of plastic deformation, cracks are easy to form and grow along the interface of matrix and WS_2 due to the weak bond between them. When these long cracks propagate to the contact surface, large flake-like debris could form, which results in the delamination wear, as shown in Fig. 11(b). In addition, as discussed earlier, sample S5 has higher bending strength, which could enhance the bond between copper and WS_2 and then restrain the nucleation and subsequent growth of cracks. As a result, the removal of materials of sample S5 is less than that of sample S0.6. Finally, sample S5 provides an excellent friction and wear performance during the process of sliding contacts.

4 Conclusions

1) The bending strength of Cu−WS_2 composites decreases from 292.2 to 181.5 MPa as the WS_2 particle size decreases from 5.0 to 0.6 μm. The analogous layered structure extremely improves the interfacial bonding strength of the composites with WS_2 particle size of 5.0 μm, which results in a higher bending strength.

2) The average friction coefficients of sample S5 and sample S0.6 are only 0.158 and 0.172, respectively. The wear rate of Cu−WS_2 composite is greatly affected by the size of WS_2 particle. The wear rate of Cu−WS_2 composite sharply increases from 2.99×10^{-14} to 6.13×10^{-14} $m^3/(N\cdot m)$ with decreasing the WS_2 particle size from 5.0 to 0.6 μm.

3) The main wear mechanism for both kinds of samples is delamination wear. The composite with smaller particle size of WS_2 has larger number of particles and higher surface energy, which is easy to react with moisture and oxygen in the environment to form tribooxidation products, resulting in higher coefficient friction and wear rate.

4) As the size of WS_2 particle increases to 5.0 μm, the size of wear debris decreases, and the transfer film is smoother and more continuous. Moreover, few extended cracks emerge on the worn subsurface of sample S5, which plays an important role in keeping the excellent wear resistance.

References

[1] KATO H, TAKAMA M, IWAI Y, WASHIDA K, SASAKI Y. Wear and mechanical properties of sintered copper−tin composites containing graphite or molybdenum disulfide [J]. Wear, 2003, 255: 573−578.

[2] ZAHRAN R R, IBRAHIM I H M, SEDAHMED G H. The corrosion of graphite/copper composites in different aqueous environments [J]. Materials Letters, 1996, 28: 237−244.

[3] LI Jing-fu, ZHANG Lei, XIAO Jin-kun, ZHOU Ke-chao. Sliding wear behavior of copper-based composites reinforced with graphene nanosheets and graphite [J]. Transactions of Nonferrous Metals Society of China, 2015, 25: 3354−3362.

[4] MALLIKARJUNA H M, KASHYAP K T, KOPPAD P G, RAMESH C S, KESHAVAMURTHY R. Microstructure and dry sliding wear behavior of Cu−Sn alloy reinforced with multiwalled carbon nanotubes [J]. Transactions of Nonferrous Metals Society of China, 2016, 26: 1755−1764.

[5] QIAN Gang, FENG Yi, CHEN Fan-yan, LIU Wen-hong, ZHANG Xue-bin, LIU Yan-fang. Effect of current polarity on electrical sliding wear behavior of Cu−WS_2−graphite−WS_2 nanotube composites in air and vacuum conditions [J]. Science China Technological Sciences, 2013, 56: 2839−2846.

[6] QIAN Gang, FENG Yi, CHEN Yang-ming, MO Fei, WANG Yu-qing, LIU Wen-hong. Effect of WS_2 addition on electrical sliding wear behaviors of Cu−graphite−WS_2 composites [J]. Transactions of Nonferrous Metals Society of China, 2015, 25: 1986−1994.

[7] HUANG Shi-ying, FENG Yi, LIU Hong-juan, DING Ke-wang, QIAN Gang. Electrical sliding friction and wear properties of Cu−MoS_2−graphite−WS_2 nanotubes composites in air and vacuum conditions [J]. Materials Science and Engineering A, 2013, 560: 685−692.

[8] WONG K C, LU X, COTTER J, EADIE D T, WONG P C. Surface and friction characterization of MoS_2, and WS_2, third body thin films under simulated wheel/rail rolling-sliding contact [J]. Wear, 2008, 264: 526−534.

[9] ZHAO Lin, YAO Ping-ping, XIAO Ye-long, TAN Hui-qiang, GONG Tai-min, ZHOU Hai-bin, ZUO Xiao-ting. Sintering behavior of WS_2 in Cu-based lead-free solid self-lubricating materials [J]. Materials Science and Engineering of Powder Metallurgy, 2013, 18: 477−482. (in Chinese)

[10] CAO Hui-quan, QIAN Zhi-yuan, ZHANG Lei, XIAO Jin-kun, ZHOU Ke-chao. Tribological behavior of Cu matrix composites containing graphite and tungsten disulfide [J]. Tribology Transactions, 2014, 57: 1037−1043.

[11] XIAO Shu-long, TIAN Jing, XU Li-juan, CHEN Yu-yong, YU Hong-bao, HAN Jie-cai. Microstructures and mechanical properties of TiAl alloy prepared by spark plasmas sintering [J]. Transactions of Nonferrous Metals Society of China, 2009, 19: 1423−1427.

[12] KOVÁČIK J, ŠTEFAN EMMER, BIELEK J. Effect of composition on friction coefficient of Cu-graphite composites [J]. Wear, 2008, 265: 417−421.

[13] RAJKUMAR K, ARAVINDAN S. Tribological behavior of microwave processed copper-nanographite composites [J]. Tribology International, 2013, 57: 282−296.

[14] BRAVUNOVIC M, KONCHITS V V, MYSHKIN N K. Electrical contacts: Fundamentals, applications and technology [M]. New York: CRC Press, 2007.

[15] SARAVANAN S D, SENTHILKUMAR M, SHANKAR S. Effect of particle size on tribological behavior of rice husk ash-reinforced aluminum alloy ($AlSi_{10}Mg$) matrix composites [J]. Tribology Transactions, 2013, 56: 1505−1513.

[16] MOUSTAFA S F, EL-BADRY S A, SANAD A M, KIEBACK B. Friction and wear of copper−graphite composites made with Cu-coated and uncoated graphite powders [J]. Wear, 2002, 253: 699−710.

[17] YASAR I, CANAKCI A, ARSLAN F. The effect of brush spring pressure on the wear behaviour of copper−graphite brushes with electrical current [J]. Tribology International, 2007, 40: 1381−1386.

[18] KESTURSATYA M, KIM J K, ROHATGI P K. Friction and wear behavior of a centrifugally cast lead-free copper alloy containing graphite particles [J]. Metallurgical and Materials Transactions A, 2001, 32: 2115−2125.
[19] RAPOPORT L, FELDMAN Y, HOMYONFER M, COHEN H, SLOAN J, HUTCHISON J. Inorganic fullerene-like material as additives to lubricants: structure-function relationship [J]. Wear, 1999, 225: 975−982.
[20] JHA A K, PRASAD S V, UPADHYAYA G S. Dry sliding wear of sintered 6061 aluminium alloy-graphite particle composites [J]. Tribology International, 1989, 22: 321−327.
[21] ZHOU Guang-wen, YANG J C. Temperature effect on the Cu_2O oxide morphology created by oxidation of Cu (001) as investigated by in situ UHV TEM [J]. Applied Surface Science, 2003, 210: 165−170.
[22] XU Yu-xi, HONG Wen-jing, BAI Hua, LI Chun, SHI Gao-quan. Strong and ductile poly(vinyl alcohol)/graphene oxide composite films with a layered structure [J]. Carbon, 2009, 47: 3538−3543.
[23] ZHANG Lei, XIAO Jin-kun, ZHOU Ke-chao. Sliding wear behavior of silver–molybdenum disulfide composite [J]. Tribology Transactions, 2012, 55: 473−480.
[24] SCHARF T W, PRASAD S V. Solid lubricants: A review [J]. Journal of Materials Science, 2013, 48: 511−531.
[25] PRASAD S V, ZABINSKI J S. Tribology of tungsten disulphide (WS_2): Characterization of wear-induced transfer films [J]. Journal of Materials Science Letters, 1993, 12: 1413−1415.
[26] SLINEY H E. Solid lubricant materials for high temperatures: A review [J]. Tribology International, 1982, 15: 303−315.
[27] ZABINSKI J S, DONLEY M S, PRASAD S V, MCDEVITT N T. Synthesis and characterization of tungsten disulphide films grown by pulsed-laser deposition [J]. Journal of Materials Science, 1994, 29: 4834−4839.
[28] FIEMING J R, SUH N P. The relationship between crack propagation rates and wear rates [J]. Wear, 1977, 44: 57−64.
[29] ZHANG J, ALPAS A T. Delamination wear in ductile materials containing second phase particles [J]. Materials Science and Engineering A, 1993, 160: 25−35.
[30] CHEN Wei, GAO Yi-min, WANG Yong, LI Huang-qiang. Tribological behavior of Si_3N_4-hBN ceramic materials without lubrication under different test modes [J]. Tribology Transactions, 2010, 53: 787−798.
[31] MA Wen-lin, LU Jin-jun. Effect of surface texture on transfer layer formation and tribological behaviour of copper–graphite composite [J]. Wear, 2011, 270: 218−229.
[32] CHEN Wu, WANG Yan, ZHANG Lei, ZHOU Ke-chao. The effect of hot extrusion on mechanical and tribological behavior of Ag−Cu/MoS_2 composites [J]. Tribology Transactions, 2015, 59: 1−36.
[33] CHEN Fan-yan, FENG Yi, SHAO Hao, ZHANG Xue-bin, CHEN Jie, CHEN Nan-nan. Friction and wear behaviors of Ag/MoS_2/G composite in different atmospheres and at different temperatures [J]. Tribology Letters, 2012, 47: 139−148.

WS_2 颗粒尺寸对放电等离子烧结 Cu−WS_2 复合材料力学和摩擦学性能的影响

周 金[1]，马 超[2]，康 潇[1]，张 雷[1]，刘新利[1]

1. 中南大学 粉末冶金国家重点实验室，长沙 410083；
2. 上海宇航系统工程研究所，上海 201109

摘 要：以 2 种不同尺寸 0.6 和 5.0 μm WS_2 和 Cu 粉为原材料，采用放电等离子烧结技术制备 Cu−WS_2 复合材料，研究 WS_2 钨颗粒尺寸对复合材料力学和摩擦学性能的影响规律。结果表明：Cu−WS_2 复合材料的抗弯强度和摩擦学性能受 WS_2 颗粒尺寸的影响较大；以 5.0 μm WS_2 颗粒为润滑相的 Cu−WS_2 复合材料的抗弯强度为 292.2 MPa；而当 WS_2 润滑相尺寸降低到 0.6 μm 时，复合材料的抗弯强度降低到 181.5 MPa。摩擦磨损试验结果表明：当润滑相 WS_2 颗粒尺寸从 5.0 μm 降到 0.6 μm 时，Cu−WS_2 复合材料的磨损率从 2.99×10^{-14} $m^3/(N\cdot m)$增大到 6.13×10^{-14} $m^3/(N\cdot m)$，且摩擦因数从 0.158 增大到 0.172。WS_2 颗粒尺寸对转移膜的形成具有重要的影响，含较大尺寸 WS_2 润滑相的 Cu−WS_2 复合材料更易在对偶盘上形成平滑且连续的转移层，这大大降低了复合材料磨损率和摩擦因数。

关键词：Cu−WS_2 复合材料；力学性能；磨损率；摩擦因数；连续转移层；放电等离子烧结

(Edited by Wei-ping CHEN)